

Search for the rare decays $B^+ \rightarrow \mu^+ \mu^- K^+$, $B^0 \rightarrow \mu^+ \mu^- K^*(892)^0$, and $B_s^0 \rightarrow \mu^+ \mu^- \phi$ at CDF

T. Aaltonen,²⁴ J. Adelman,¹⁴ T. Akimoto,⁵⁶ M. G. Albrow,¹⁸ B. Álvarez González,¹² S. Amerio,^{44a,44b} D. Amidei,³⁵ A. Anastassov,³⁹ A. Annovi,²⁰ J. Antos,¹⁵ G. Apollinari,¹⁸ A. Apresyan,⁴⁹ T. Arisawa,⁵⁸ A. Artikov,¹⁶ W. Ashmanskas,¹⁸ A. Attal,⁴ A. Aurisano,⁵⁴ F. Azfar,⁴³ P. Azzurri,^{47a,47d} W. Badgett,¹⁸ A. Barbaro-Galtieri,²⁹ V. E. Barnes,⁴⁹ B. A. Barnett,²⁶ V. Bartsch,³¹ G. Bauer,³³ P.-H. Beauchemin,³⁴ F. Bedeschi,^{47a} P. Bednar,¹⁵ D. Beecher,³¹ S. Behari,²⁶ G. Bellettini,^{47a,47b} J. Bellinger,⁶⁰ D. Benjamin,¹⁷ A. Beretvas,¹⁸ J. Beringer,²⁹ A. Bhatti,⁵¹ M. Binkley,¹⁸ D. Bisello,^{44a,44b} I. Bizjak,³¹ R. E. Blair,² C. Blocker,⁷ B. Blumenfeld,²⁶ A. Bocci,¹⁷ A. Bodek,⁵⁰ V. Boisvert,⁵⁰ G. Bolla,⁴⁹ D. Bortoletto,⁴⁹ J. Boudreau,⁴⁸ A. Boveia,¹¹ B. Brau,¹¹ A. Bridgeman,²⁵ L. Brigliadori,^{44a} C. Bromberg,³⁶ E. Brubaker,¹⁴ J. Budagov,¹⁶ H. S. Budd,⁵⁰ S. Budd,²⁵ K. Burkett,¹⁸ G. Busetto,^{44a,44b} P. Bussey,^{22,r} A. Buzatu,³⁴ K. L. Byrum,² S. Cabrera,^{17,q} C. Calancha,³² M. Campanelli,³⁶ M. Campbell,³⁵ F. Canelli,¹⁸ A. Canepa,⁴⁶ D. Carlsmith,⁶⁰ R. Carosi,^{47a} S. Carrillo,^{19,k} S. Carron,³⁴ B. Casal,¹² M. Casarsa,¹⁸ A. Castro,^{6a,6b} P. Catastini,^{47a,47c} D. Cauz,^{55a,55b} V. Cavaliere,^{47a,47c} M. Cavalli-Sforza,⁴ A. Cerri,²⁹ L. Cerrito,^{31,o} S. H. Chang,²⁸ Y. C. Chen,¹ M. Chertok,⁸ G. Chiarelli,^{47a} G. Chlachidze,¹⁸ F. Chlebana,¹⁸ K. Cho,²⁸ D. Chokheli,¹⁶ J. P. Chou,²³ G. Choudalakis,³³ S. H. Chuang,⁵³ K. Chung,¹³ W. H. Chung,⁶⁰ Y. S. Chung,⁵⁰ C. I. Ciobanu,⁴⁵ M. A. Ciocci,^{47a,47c} A. Clark,²¹ D. Clark,⁷ G. Compostella,^{44a} M. E. Convery,¹⁸ J. Conway,⁸ K. Copic,³⁵ M. Cordelli,²⁰ G. Cortiana,^{44a,44b} D. J. Cox,⁸ F. Crescioli,^{47a,47b} C. Cuenca Almenar,^{8,q} J. Cuevas,^{12,n} R. Culbertson,¹⁸ J. C. Cully,³⁵ D. Dagenhart,¹⁸ M. Datta,¹⁸ T. Davies,²² P. de Barbaro,⁵⁰ S. De Cecco,^{52a} A. Deisher,²⁹ G. De Lorenzo,⁴ M. Dell'Orso,^{47a,47b} C. Deluca,⁴ L. Demortier,⁵¹ J. Deng,¹⁷ M. Deninno,^{6a} P. F. Derwent,¹⁸ G. P. di Giovanni,⁴⁵ C. Dionisi,^{52a,52b} B. Di Ruzza,^{55a,55b} J. R. Dittmann,⁵ M. D'Onofrio,⁴ S. Donati,^{47a,47b} P. Dong,⁹ J. Donini,^{44a} T. Dorigo,^{44a} S. Dube,⁵³ J. Efron,⁴⁰ A. Elagin,⁵⁴ R. Erbacher,⁸ D. Errede,²⁵ S. Errede,²⁵ R. Eusebi,¹⁸ H. C. Fang,²⁹ S. Farrington,⁴³ W. T. Fedorko,¹⁴ R. G. Feild,⁶¹ M. Feindt,²⁷ J. P. Fernandez,³² C. Ferrazza,^{47a,47d} R. Field,¹⁹ G. Flanagan,⁴⁹ R. Forrest,⁸ M. Franklin,²³ J. C. Freeman,¹⁸ I. Furic,¹⁹ M. Gallinaro,^{52a} J. Galyardt,¹³ F. Garbersson,¹¹ J. E. Garcia,^{47a} A. F. Garfinkel,⁴⁹ K. Genser,¹⁸ H. Gerberich,²⁵ D. Gerdes,³⁵ A. Gessler,²⁷ S. Giagu,^{52a,52b} V. Giakoumopoulou,³ P. Giannetti,^{47a} K. Gibson,⁴⁸ J. L. Gimmell,⁵⁰ C. M. Ginsburg,¹⁸ N. Giokaris,³ M. Giordani,^{55a,55b} P. Giromini,²⁰ M. Giunta,^{47a,47b} G. Giurgiu,²⁶ V. Glagolev,¹⁶ D. Glenzinski,¹⁸ M. Gold,³⁸ N. Goldschmidt,¹⁹ A. Golossanov,¹⁸ G. Gomez,¹² G. Gomez-Ceballos,³³ M. Goncharov,⁵⁴ O. González,³² I. Gorelov,³⁸ A. T. Goshaw,¹⁷ K. Goulianos,⁵¹ A. Gresele,^{44a,44b} S. Grinstein,²³ C. Grosso-Pilcher,¹⁴ R. C. Group,¹⁸ U. Grundler,²⁵ J. Guimaraes da Costa,²³ Z. Gunay-Unalan,³⁶ C. Haber,²⁹ K. Hahn,³³ S. R. Hahn,¹⁸ E. Halkiadakis,⁵³ B.-Y. Han,⁵⁰ J. Y. Han,⁵⁰ R. Handler,⁶⁰ F. Happacher,²⁰ K. Hara,⁵⁶ D. Hare,⁵³ M. Hare,⁵⁷ S. Harper,⁴³ R. F. Harr,⁵⁹ R. M. Harris,¹⁸ M. Hartz,⁴⁸ K. Hatakeyama,⁵¹ J. Hauser,⁹ C. Hays,⁴³ M. Heck,²⁷ A. Heijboer,⁴⁶ B. Heinemann,²⁹ J. Heinrich,⁴⁶ C. Henderson,³³ M. Herndon,⁶⁰ J. Heuser,²⁷ S. Hewamanage,⁵ D. Hidas,¹⁷ C. S. Hill,^{11,d} D. Hirschbuehl,²⁷ A. Hocker,¹⁸ S. Hou,¹ M. Houlden,³⁰ S.-C. Hsu,¹⁰ B. T. Huffman,⁴³ R. E. Hughes,⁴⁰ U. Husemann,⁶¹ J. Huston,³⁶ J. Incandela,¹¹ G. Introzzi,^{47a} M. Iori,^{52a,52b} A. Ivanov,⁸ E. James,¹⁸ B. Jayatilaka,¹⁷ E. J. Jeon,²⁸ M. K. Jha,^{6a} S. Jindariani,¹⁸ W. Johnson,⁸ M. Jones,⁴⁹ K. K. Joo,²⁸ S. Y. Jun,¹³ J. E. Jung,²⁸ T. R. Junk,¹⁸ T. Kamon,⁵⁴ D. Kar,¹⁹ P. E. Karchin,⁵⁹ Y. Kato,⁴² R. Kephart,¹⁸ J. Keung,⁴⁶ V. Khotilovich,⁵⁴ B. Kilminster,⁴⁰ D. H. Kim,²⁸ H. S. Kim,²⁸ J. E. Kim,²⁸ M. J. Kim,²⁰ S. B. Kim,²⁸ S. H. Kim,⁵⁶ Y. K. Kim,¹⁴ N. Kimura,⁵⁶ L. Kirsch,⁷ S. Klimenko,¹⁹ B. Knuteson,³³ B. R. Ko,¹⁷ S. A. Koay,¹¹ K. Kondo,⁵⁸ D. J. Kong,²⁸ J. Konigsberg,¹⁹ A. Korytov,¹⁹ A. V. Kotwal,¹⁷ M. Kreps,²⁷ J. Kroll,⁴⁶ N. Krumnack,⁵ M. Kruse,¹⁷ V. Krutelyov,¹¹ T. Kubo,⁵⁶ T. Kuhr,²⁷ N. P. Kulkarni,⁵⁹ M. Kurata,⁵⁶ Y. Kusakabe,⁵⁸ S. Kwang,¹⁴ A. T. Laasanen,⁴⁹ S. Lami,^{47a} S. Lammel,¹⁸ M. Lancaster,³¹ R. L. Lander,⁸ K. Lannon,⁴⁰ A. Lath,⁵³ G. Latino,^{47a,47c} I. Lazzizzera,^{44a,44b} T. LeCompte,² E. Lee,⁵⁴ S. W. Lee,^{54,p} S. Leone,^{47a} S. Levy,¹⁴ J. D. Lewis,¹⁸ C. S. Lin,²⁹ J. Linacre,⁴³ M. Lindgren,¹⁸ E. Lipeles,¹⁰ A. Lister,⁸ D. O. Litvintsev,¹⁸ C. Liu,⁴⁸ T. Liu,¹⁸ N. S. Lockyer,⁴⁶ A. Loginov,⁶¹ M. Loretì,^{44a,44b} L. Lovas,¹⁵ R.-S. Lu,¹ D. Lucchesi,^{44a,44b} J. Lueck,²⁷ C. Luci,^{52a,52b} P. Lujan,²⁹ P. Lukens,¹⁸ G. Lungu,⁵¹ L. Lyons,⁴³ J. Lys,²⁹ R. Lysak,¹⁵ E. Lytken,⁴⁹ P. Mack,²⁷ D. MacQueen,³⁴ R. Madrak,¹⁸ K. Maeshima,¹⁸ K. Makhoul,³³ T. Maki,²⁴ P. Maksimovic,²⁶ S. Malde,⁴³ S. Malik,³¹ G. Manca,³⁰ A. Manousakis-Katsikakis,³ F. Margaroli,⁴⁹ C. Marino,²⁷ C. P. Marino,²⁵ A. Martin,⁶¹ V. Martin,^{22,j} M. Martínez,⁴ R. Martínez-Ballarín,³² T. Maruyama,⁵⁶ P. Mastrandrea,^{52a} T. Masubuchi,⁵⁶ M. E. Mattson,⁵⁹ P. Mazzanti,^{6a} K. S. McFarland,⁵⁰ P. McIntyre,⁵⁴ R. McNulty,^{30,i} A. Mehta,³⁰ P. Mehtala,²⁴ A. Menzione,^{47a} P. Merkel,⁴⁹ C. Mesropian,⁵¹ T. Miao,¹⁸ N. Miladinovic,⁷ R. Miller,³⁶ C. Mills,²³ M. Milnik,²⁷ A. Mitra,¹ G. Mitselmakher,¹⁹ H. Miyake,⁵⁶ N. Moggi,^{6a} C. S. Moon,²⁸ R. Moore,¹⁸ M. J. Morello,^{47a,47b} J. Morlok,²⁷ P. Movilla Fernandez,¹⁸ J. Mülmenstädt,²⁹ A. Mukherjee,¹⁸ Th. Müller,²⁷ R. Mumford,²⁶ P. Murat,¹⁸ M. Mussini,^{6a,6b} J. Nachtman,¹⁸ Y. Nagai,⁵⁶ A. Nagano,⁵⁶ J. Naganoma,⁵⁸ K. Nakamura,⁵⁶ I. Nakano,⁴¹ A. Napier,⁵⁷ V. Necula,¹⁷ C. Neu,⁴⁶ M. S. Neubauer,²⁵ J. Nielsen,^{29,f} L. Nodulman,² M. Norman,¹⁰ O. Norniella,²⁵ E. Nurse,³¹

L. Oakes,⁴³ S. H. Oh,¹⁷ Y. D. Oh,²⁸ I. Oksuzian,¹⁹ T. Okusawa,⁴² R. Oldeman,³⁰ R. Orava,²⁴ K. Osterberg,²⁴ S. Pagan Griso,^{44a,44b} C. Pagliarone,^{47a} E. Palencia,¹⁸ V. Papadimitriou,¹⁸ A. Papaikonomou,²⁷ A. A. Paramonov,¹⁴ B. Parks,⁴⁰ S. Pashapour,³⁴ J. Patrick,¹⁸ G. Pauletta,^{55a,55b} M. Paulini,¹³ C. Paus,³³ D. E. Pellett,⁸ A. Penzo,^{55a} T. J. Phillips,¹⁷ G. Piacentino,^{47a} E. Pianori,⁴⁶ L. Pinera,¹⁹ K. Pitts,²⁵ C. Plager,⁹ L. Pondrom,⁶⁰ O. Poukhov,¹⁶ N. Pounder,⁴³ F. Prakoashyn,¹⁶ A. Pronko,¹⁸ J. Proudfoot,² F. Ptohos,^{18,h} E. Pueschel,¹³ G. Punzi,^{47a,47b} J. Pursley,⁶⁰ J. Rademacker,^{43,d} A. Rahaman,⁴⁸ V. Ramakrishnan,⁶⁰ N. Ranjan,⁴⁹ I. Redondo,³² B. Reiserer,¹⁸ V. Rekovic,³⁸ P. Renton,⁴³ M. Rescigno,^{52a} S. Richter,²⁷ F. Rimondi,^{6a,6b} L. Ristori,^{47a} A. Robson,²² T. Rodrigo,¹² T. Rodriguez,⁴⁶ E. Rogers,²⁵ S. Rolli,⁵⁷ R. Roser,¹⁸ M. Rossi,^{55a} R. Rossin,¹¹ P. Roy,³⁴ A. Ruiz,¹² J. Russ,¹³ V. Rusu,¹⁸ H. Saarikko,²⁴ A. Safonov,⁵⁴ W. K. Sakumoto,⁵⁰ O. Saltó,⁴ L. Santi,^{55a,55b} S. Sarkar,^{52a,52b} L. Sartori,^{47a} K. Sato,¹⁸ A. Savoy-Navarro,⁴⁵ T. Scheidle,²⁷ P. Schlabach,¹⁸ A. Schmidt,²⁷ E. E. Schmidt,¹⁸ M. A. Schmidt,¹⁴ M. P. Schmidt,^{61,a} M. Schmitt,³⁹ T. Schwarz,⁸ L. Scodellaro,¹² A. L. Scott,¹¹ A. Scribano,^{47a,47c} F. Scuri,^{47a} A. Sedov,⁴⁹ S. Seidel,³⁸ Y. Seiya,⁴² A. Semenov,¹⁶ L. Sexton-Kennedy,¹⁸ A. Sfyrla,²¹ S. Z. Shalhout,⁵⁹ T. Shears,³⁰ P. F. Shepard,⁴⁸ D. Sherman,²³ M. Shimojima,^{56,m} S. Shiraishi,¹⁴ M. Shochet,¹⁴ Y. Shon,⁶⁰ I. Shreyber,³⁷ A. Sidoti,^{47a} P. Sinervo,³⁴ A. Sisakyan,¹⁶ A. J. Slaughter,¹⁸ J. Slaunwhite,⁴⁰ K. Sliwa,⁵⁷ J. R. Smith,⁸ F. D. Snider,¹⁸ R. Snihur,³⁴ A. Soha,⁸ S. Somalwar,⁵³ V. Sorin,³⁶ J. Spalding,¹⁸ T. Spreitzer,³⁴ P. Squillacioti,^{47a,47c} M. Stanitzki,⁶¹ R. St. Denis,²² B. Stelzer,⁹ O. Stelzer-Chilton,⁴³ D. Stentz,³⁹ J. Strologas,³⁸ D. Stuart,¹¹ J. S. Suh,²⁸ A. Sukhanov,¹⁹ I. Suslov,¹⁶ T. Suzuki,⁵⁶ A. Taffard,^{25,e} R. Takashima,⁴¹ Y. Takeuchi,⁵⁶ R. Tanaka,⁴¹ M. Tecchio,³⁵ P. K. Teng,¹ K. Terashi,⁵¹ R. J. Tesarek,¹⁸ J. Thom,^{18,g} A. S. Thompson,²² G. A. Thompson,²⁵ E. Thomson,⁴⁶ P. Tipton,⁶¹ V. Tiwari,¹³ S. Tkaczyk,¹⁸ D. Toback,⁵⁴ S. Tokar,¹⁵ K. Tollefson,³⁶ T. Tomura,⁵⁶ D. Tonelli,¹⁸ S. Torre,²⁰ D. Torretta,¹⁸ P. Totaro,^{55a,55b} S. Tourneur,⁴⁵ Y. Tu,⁴⁶ N. Turini,^{47a,47c} F. Ukegawa,⁵⁶ S. Vallecorsa,²¹ N. van Remortel,^{24,b} A. Varganov,³⁵ E. Vataga,^{47a,47d} F. Vázquez,^{19,k} G. Velev,¹⁸ C. Vellidis,³ V. Veszpremi,⁴⁹ M. Vidal,³² R. Vidal,¹⁸ I. Vila,¹² R. Vilar,¹² T. Vine,³¹ M. Vogel,³⁸ I. Volobouev,^{29,p} G. Volpi,^{47a,47b} F. Würthwein,¹⁰ P. Wagner,² R. G. Wagner,² R. L. Wagner,¹⁸ J. Wagner-Kuhr,²⁷ W. Wagner,²⁷ T. Wakisaka,⁴² R. Wallny,⁹ S. M. Wang,¹ A. Warburton,³⁴ D. Waters,³¹ M. Weinberger,⁵⁴ W. C. Wester III,¹⁸ B. Whitehouse,⁵⁷ D. Whiteson,^{46,e} A. B. Wicklund,² E. Wicklund,¹⁸ G. Williams,³⁴ H. H. Williams,⁴⁶ P. Wilson,¹⁸ B. L. Winer,⁴⁰ P. Wittich,^{18,g} S. Wolbers,¹⁸ C. Wolfe,¹⁴ T. Wright,³⁵ X. Wu,²¹ S. M. Wynne,³⁰ A. Yagil,¹⁰ K. Yamamoto,⁴² J. Yamaoka,⁵³ U. K. Yang,^{14,l} Y. C. Yang,²⁸ W. M. Yao,²⁹ G. P. Yeh,¹⁸ J. Yoh,¹⁸ K. Yorita,¹⁴ T. Yoshida,⁴² G. B. Yu,⁵⁰ I. Yu,²⁸ S. S. Yu,¹⁸ J. C. Yun,¹⁸ L. Zanello,^{52a,52b} A. Zanetti,^{55a} I. Zaw,²³ X. Zhang,²⁵ Y. Zheng,^{9,c} and S. Zucchelli^{6a,6b}

(CDF Collaboration)

¹*Institute of Physics, Academia Sinica, Taipei, Taiwan 11529, Republic of China*²*Argonne National Laboratory, Argonne, Illinois 60439*³*University of Athens, 157 71 Athens, Greece*⁴*Institut de Física d'Altes Energies, Universitat Autònoma de Barcelona, E-08193, Bellaterra (Barcelona), Spain*⁵*Baylor University, Waco, Texas 76798*^{6a}*Istituto Nazionale di Fisica Nucleare Bologna, I-40127 Bologna, Italy*^{6b}*University of Bologna, I-40127 Bologna, Italy*⁷*Brandeis University, Waltham, Massachusetts 02254*⁸*University of California, Davis, Davis, California 95616*⁹*University of California, Los Angeles, Los Angeles, California 90024*¹⁰*University of California, San Diego, La Jolla, California 92093*¹¹*University of California, Santa Barbara, Santa Barbara, California 93106*¹²*Instituto de Física de Cantabria, CSIC-University of Cantabria, 39005 Santander, Spain*¹³*Carnegie Mellon University, Pittsburgh, Pennsylvania 15213*¹⁴*Enrico Fermi Institute, University of Chicago, Chicago, Illinois 60637*¹⁵*Comenius University, 842 48 Bratislava, Slovakia; Institute of Experimental Physics, 040 01 Kosice, Slovakia*¹⁶*Joint Institute for Nuclear Research, RU-141980 Dubna, Russia*¹⁷*Duke University, Durham, North Carolina 27708*¹⁸*Fermi National Accelerator Laboratory, Batavia, Illinois 60510*¹⁹*University of Florida, Gainesville, Florida 32611*²⁰*Laboratori Nazionali di Frascati, Istituto Nazionale di Fisica Nucleare, I-00044 Frascati, Italy*²¹*University of Geneva, CH-1211 Geneva 4, Switzerland*²²*Glasgow University, Glasgow G12 8QQ, United Kingdom*²³*Harvard University, Cambridge, Massachusetts 02138*

- ²⁴*Division of High Energy Physics, Department of Physics, University of Helsinki and Helsinki Institute of Physics, FIN-00014, Helsinki, Finland*
- ²⁵*University of Illinois, Urbana, Illinois 61801*
- ²⁶*The Johns Hopkins University, Baltimore, Maryland 21218*
- ²⁷*Institut für Experimentelle Kernphysik, Universität Karlsruhe, 76128 Karlsruhe, Germany*
- ²⁸*Center for High Energy Physics: Kyungpook National University, Daegu 702-701, Korea; Seoul National University, Seoul 151-742, Korea; Sungkyunkwan University, Suwon 440-746, Korea; Korea Institute of Science and Technology Information, Daejeon, 305-806, Korea; Chonnam National University, Gwangju, 500-757, Korea*
- ²⁹*Ernest Orlando Lawrence Berkeley National Laboratory, Berkeley, California 94720*
- ³⁰*University of Liverpool, Liverpool L69 7ZE, United Kingdom*
- ³¹*University College London, London WC1E 6BT, United Kingdom*
- ³²*Centro de Investigaciones Energeticas Medioambientales y Tecnologicas, E-28040 Madrid, Spain*
- ³³*Massachusetts Institute of Technology, Cambridge, Massachusetts 02139*
- ³⁴*Institute of Particle Physics: McGill University, Montréal, Canada H3A 2T8; and University of Toronto, Toronto, Canada M5S 1A7*
- ³⁵*University of Michigan, Ann Arbor, Michigan 48109*
- ³⁶*Michigan State University, East Lansing, Michigan 48824*
- ³⁷*Institution for Theoretical and Experimental Physics, ITEP, Moscow 117259, Russia*
- ³⁸*University of New Mexico, Albuquerque, New Mexico 87131*
- ³⁹*Northwestern University, Evanston, Illinois 60208*
- ⁴⁰*The Ohio State University, Columbus, Ohio 43210*
- ⁴¹*Okayama University, Okayama 700-8530, Japan*
- ⁴²*Osaka City University, Osaka 588, Japan*
- ⁴³*University of Oxford, Oxford OX1 3RH, United Kingdom*
- ^{44a}*Istituto Nazionale di Fisica Nucleare, Sezione di Padova-Trento, I-35131 Padova, Italy*
- ^{44b}*University of Padova, I-35131 Padova, Italy*
- ⁴⁵*LPNHE, Université Pierre et Marie Curie/IN2P3-CNRS, UMR7585, Paris, F-75252 France*
- ⁴⁶*University of Pennsylvania, Philadelphia, Pennsylvania 19104*
- ^{47a}*Istituto Nazionale di Fisica Nucleare Pisa, I-56127 Pisa, Italy;*
- ^{47b}*University of Pisa, I-56127 Pisa, Italy*
- ^{47c}*University of Siena, I-56127 Pisa, Italy*
- ^{47d}*Scuola Normale Superiore, I-56127 Pisa, Italy*
- ⁴⁸*University of Pittsburgh, Pittsburgh, Pennsylvania 15260*
- ⁴⁹*Purdue University, West Lafayette, Indiana 47907*
- ⁵⁰*University of Rochester, Rochester, New York 14627*
- ⁵¹*The Rockefeller University, New York, New York 10021*
- ^{52a}*Istituto Nazionale di Fisica Nucleare, Sezione di Roma 1, I-00185 Roma, Italy*
- ^{52b}*Sapienza Università di Roma, I-00185 Roma, Italy*

^aDeceased.

^bVisitors from Universiteit Antwerpen, B-2610 Antwerp, Belgium.

^cVisitors from Chinese Academy of Sciences, Beijing 100864, China.

^dVisitors from University of Bristol, Bristol BS8 1TL, United Kingdom.

^eVisitors from University of California Irvine, Irvine, CA 92697, USA.

^fVisitors from University of California Santa Cruz, Santa Cruz, CA 95064, USA.

^gVisitors from Cornell University, Ithaca, NY 14853, USA.

^hVisitors from University of Cyprus, Nicosia CY-1678, Cyprus.

ⁱVisitors from University College Dublin, Dublin 4, Ireland.

^jVisitors from University of Edinburgh, Edinburgh EH9 3JZ, United Kingdom.

^kVisitors from Universidad Iberoamericana, Mexico D.F., Mexico.

^lVisitors from University of Manchester, Manchester M13 9PL, England.

^mVisitors from Nagasaki Institute of Applied Science, Nagasaki, Japan.

ⁿVisitors from University de Oviedo, E-33007 Oviedo, Spain.

^oVisitors from Queen Mary, University of London, London, E1 4NS, England.

^pVisitors from Texas Tech University, Lubbock, TX 79409, USA.

^qVisitors from IFIC (CSIC-Universitat de Valencia), 46071 Valencia, Spain.

^rVisitors from Royal Society of Edinburgh/Scottish Executive Support Research Fellow.

⁵³*Rutgers University, Piscataway, New Jersey 08855*⁵⁴*Texas A&M University, College Station, Texas 77843*^{55a}*Istituto Nazionale di Fisica Nucleare Trieste/Udine, Udine, Italy*^{55b}*University of Trieste/Udine, Udine, Italy*⁵⁶*University of Tsukuba, Tsukuba, Ibaraki 305, Japan*⁵⁷*Tufts University, Medford, Massachusetts 02155*⁵⁸*Waseda University, Tokyo 169, Japan*⁵⁹*Wayne State University, Detroit, Michigan 48201*⁶⁰*University of Wisconsin, Madison, Wisconsin 53706*⁶¹*Yale University, New Haven, Connecticut 06520*

(Received 25 April 2008; published 22 January 2009)

We search for $b \rightarrow s\mu^+\mu^-$ transitions in B meson (B^+ , B^0 , or B_s^0) decays with 924 pb^{-1} of $p\bar{p}$ collisions at $\sqrt{s} = 1.96 \text{ TeV}$ collected with the CDF II detector at the Fermilab Tevatron. We find excesses with significances of 4.5, 2.9, and 2.4 standard deviations in the $B^+ \rightarrow \mu^+\mu^-K^+$, $B^0 \rightarrow \mu^+\mu^-K^*(892)^0$, and $B_s^0 \rightarrow \mu^+\mu^-\phi$ decay modes, respectively. Using $B \rightarrow J/\psi h$ ($h = K^+$, $K^*(892)^0$, ϕ) decays as normalization channels, we report branching fractions for the previously observed B^+ and B^0 decays, $\mathcal{B}(B^+ \rightarrow \mu^+\mu^-K^+) = (0.59 \pm 0.15 \pm 0.04) \times 10^{-6}$, and $\mathcal{B}(B^0 \rightarrow \mu^+\mu^-K^*(892)^0) = (0.81 \pm 0.30 \pm 0.10) \times 10^{-6}$, where the first uncertainty is statistical, and the second is systematic. We set an upper limit on the relative branching fraction $\mathcal{B}(B_s^0 \rightarrow \mu^+\mu^-\phi)/\mathcal{B}(B_s^0 \rightarrow J/\psi\phi) < 2.6(2.3) \times 10^{-3}$ at the 95(90)% confidence level, which is the most stringent to date.

DOI: 10.1103/PhysRevD.79.011104

PACS numbers: 13.20.He, 12.15.Mm, 14.40.Nd

The decay of a b quark into an s quark and two muons ($b \rightarrow s\mu^+\mu^-$) is a flavor-changing neutral current process, forbidden at tree level in the standard model (SM) but allowed through highly suppressed internal loops. New physics could manifest itself in a larger branching fraction, a modified dimuon mass distribution, or angular distributions of the decay products different from that predicted by the SM [1–4]. In this paper, we report branching ratio measurements of exclusive decays, where the s quark hadronizes into a single meson. Reconstructing a final state with only three or four charged final state particles results in smaller backgrounds than those expected in a search for inclusive $B \rightarrow X_s\mu^+\mu^-$ decays. The rare decays $B^+ \rightarrow \mu^+\mu^-K^+$ and $B^0 \rightarrow \mu^+\mu^-K^*(892)^0$ have been observed at the B factories [5,6], with branching fractions of $O(10^{-6})$, consistent with SM predictions [7–14]. The analogous decay in the B_s^0 system, $B_s^0 \rightarrow \mu^+\mu^-\phi$, has a predicted branching ratio of 1.6×10^{-6} [15], but has not yet been observed [16,17]. We report branching ratio measurements from 924 pb^{-1} of Collider Detector at Fermilab (CDF) Run II data that pave the way for future studies of larger data sets from which kinematic distributions may be measured. We search for $B \rightarrow \mu^+\mu^-h$ decays, where B stands for B^+ , B^0 , or B_s^0 , and h stands for K^+ , $K^*(892)^0$, or ϕ , respectively. The $K^*(892)^0$, referred to as K^{*0} throughout this paper, is reconstructed in the $K^{*0} \rightarrow K^+\pi^-$ decay mode, and the ϕ meson is reconstructed as $\phi \rightarrow K^+K^-$. We measure branching ratios relative to $B \rightarrow J/\psi h$ decays, followed by $J/\psi \rightarrow \mu^+\mu^-$ decays, resulting in the same final state particles as the rare decay modes. Many systematic uncertainties cancel in the relative branching ratios:

$$\frac{\mathcal{B}(B \rightarrow \mu^+\mu^-h)}{\mathcal{B}(B \rightarrow J/\psi h)} = \frac{N_{\mu^+\mu^-h}}{N_{J/\psi h}} \frac{\epsilon_{J/\psi h}}{\epsilon_{\mu^+\mu^-h}} \times \mathcal{B}(J/\psi \rightarrow \mu^+\mu^-), \quad (1)$$

where $N_{\mu^+\mu^-h}$ is the observed number of $B \rightarrow \mu^+\mu^-h$ decays, $N_{J/\psi h}$ is the observed number of $B \rightarrow J/\psi h$ decays, while $\epsilon_{J/\psi h}$ and $\epsilon_{\mu^+\mu^-h}$ are the combined selection efficiency and acceptance of the experiment for $B \rightarrow J/\psi h$ and $B \rightarrow \mu^+\mu^-h$ respectively. Throughout this report, charge conjugate modes are implicitly included.

CDF II is a general purpose detector, located at the Tevatron $p\bar{p}$ collider [18]. Charged particle trajectories (tracks) are detected by the tracking system comprised of a seven-layer double-sided silicon microstrip detector and a drift chamber, both in a 1.4 T axial magnetic field. The silicon detector [19] ranges in radius from 1.3 to 28 cm, and has a single-hit resolution of approximately $15 \mu\text{m}$. The drift chamber [20] provides up to 96 measurements from radii of 40 to 137 cm with a single-hit resolution of approximately $180 \mu\text{m}$. A muon chamber identification system of plastic scintillators and drift chambers [21] is located on the exterior of the detector with a central part covering $|\eta| < 0.6$, and an extended region covering $0.6 < |\eta| < 1.0$, where η is the pseudorapidity [22]. In the central (extended) region, muons are detected if their transverse momentum component p_T is greater than $1.5(2.0) \text{ GeV}/c$. Events are selected with a three-level trigger system. The first trigger level requires the presence of two charged particles with $p_T \geq 1.5 \text{ GeV}/c$ ($|\eta| \leq 0.6$) or $p_T \geq 2.0 \text{ GeV}/c$ ($0.6 \leq |\eta| \leq 1.0$), matched to track segments in the muon chambers to form muon candidates.

At the second level, a more restrictive selection is made by requiring that the muon candidates have opposite charge, and that their opening angle in the plane transverse to the beam line is less than 120° . At the third trigger level, the event is fully reconstructed. The trajectories of the muon candidates in the silicon detector are required to intersect at a point which is displaced transversely from the beam line by at least $100 \mu\text{m}$.

The off-line selection begins with a suppression of random combinations of tracks satisfying the selection requirements (combinatoric background), by requiring that all tracks have $p_T > 0.4 \text{ GeV}/c$ and match hits from at least three layers of the silicon detector. The trajectories of a pair of muon candidates that satisfy the trigger requirements, and the tracks that form the hadron candidate, are fitted with the constraint that they originate from a single vertex in three-dimensional space to form a B candidate. The χ^2 probability of the fit is required to be greater than 10^{-3} . A K^+ candidate is a track assigned the charged kaon mass, and the K^{*0} (ϕ) candidates are formed from oppositely charged pairs of tracks whose invariant mass must lie within $50(10) \text{ MeV}/c^2$ of the K^{*0} (ϕ) mass. For all particles, we use the world average values tabulated in Ref. [23]. The ambiguity of the mass assignment in $B^0 \rightarrow \mu^+ \mu^- K^{*0}$ decays is handled by choosing the combination whose $K^+ \pi^-$ mass is closer to the K^{*0} mass. In reconstructing the B candidates, the meson containing a strange quark h is required to have $p_T(h) \geq 1.0 \text{ GeV}/c$, and the B candidate is required to have $p_T(B) \geq 4.0 \text{ GeV}/c$. We require that the distance of closest approach between the flight path of the B candidate and the beam line, $|d_0(B)|$, is less than $120 \mu\text{m}$, to reduce the combinatoric background with no loss of signal.

Normalization mode candidates are identified by having a dimuon invariant mass within $50 \text{ MeV}/c^2$ of the J/ψ mass, yielding approximately $12000 B^+ \rightarrow J/\psi K^+$, $4400 B^0 \rightarrow J/\psi K^{*0}$, and $800 B_s^0 \rightarrow J/\psi \phi$ decays. The B candidate mass distributions of all modes are compatible with a Gaussian of width $\sigma = 20 \text{ MeV}/c^2$. To reduce backgrounds from B decays to mesons containing c quarks, several vetoes are applied to $B \rightarrow \mu^+ \mu^- h$ candidates, listed below. We eliminate candidates with a dimuon mass near the $J/\psi^{(l)}$: $2.9 \leq m_{\mu\mu} \leq 3.2 \text{ GeV}/c^2$ or $3.6 \leq m_{\mu\mu} \leq 3.75 \text{ GeV}/c^2$ respectively. $B \rightarrow J/\psi^{(l)} h$ decays followed by the radiative decay of the $J/\psi^{(l)}$ into two muons and a photon that is not reconstructed may have a dimuon mass that passes the $J/\psi^{(l)}$ veto. We reject these events making use of the correlation between the candidate's invariant mass and the dimuon invariant mass, and require $|(m_{\mu\mu h} - m_B) - (m_{\mu\mu} - m_{J/\psi^{(l)}})| > 100 \text{ MeV}/c^2$. $B \rightarrow J/\psi^{(l)} h$ decays with one hadron misidentified as a muon form a potential background to the rare decay search. We reject this class of background by requiring that all combinations of tracks of the candidate have an invariant mass that differs by at least $40 \text{ MeV}/c^2$

from the $J/\psi^{(l)}$ mass. We also reject candidates with track pairs with a mass within $\pm 25 \text{ MeV}/c^2$ of the $D^0 \rightarrow K^- \pi^+$ decay, or track triplets compatible with a mass within $\pm 25 \text{ MeV}/c^2$ of the $D^+ \rightarrow K^- \pi^+ \pi^+$ or $D_s^+ \rightarrow K^+ K^- \pi^+$ decays.

We further improve the signal to background ratio by an optimization of the selection based on discriminating variables. For this purpose, Monte Carlo (MC) simulations of the signal processes are used. We generate single b hadrons using the transverse momentum spectrum from $B \rightarrow J/\psi X$, measured by CDF [18]. Decays of all b hadrons are simulated using EVTGEN [24], with lifetimes from Ref. [23], allowing for a decay width difference between the B_s^0 mass eigenstates, $\Delta\Gamma/\Gamma = 0.12 \pm 0.06$ [25]. The decays $B^0 \rightarrow J/\psi K^{*0}$ and $B_s^0 \rightarrow J/\psi \phi$ are simulated according to the polarization amplitudes measured by CDF [26]. The dynamics of the rare decay processes are simulated according to the calculations of Ali *et al.* [11]. For $B_s^0 \rightarrow \mu^+ \mu^- \phi$, we assume a mixture of 50% CP -even and 50% CP -odd states. The interactions of final state particles are simulated using a GEANT [27] model of the CDF II detector, digitized into the CDF event format, and reconstructed using the same software as in the processing of collision data. The detector simulation includes a full emulation of the CDF trigger system. We find that the transverse momentum spectrum of the B mesons of this measurement are on average higher than in the simulation. This can be explained by the presence of a B baryon component with low transverse momentum in the measurement used as input spectrum of the simulation [18]. To correct for this, the simulated events are weighted by a polynomial function, which is obtained from the ratio of data to MC transverse momentum distribution of the B meson.

We tighten the candidate selection to obtain the smallest expected statistical uncertainty on the measurement of the $B \rightarrow \mu^+ \mu^- h$ branching ratios by finding the selection with the largest value of $N_{\text{sig}}/\sqrt{N_{\text{sig}} + N_{\text{bkg}}}$. The expected number of signal events N_{sig} is determined by scaling the MC yields of the rare decay modes to the yields of the normalization channels in the data, and correcting by the relative branching ratios and selection efficiencies. This procedure requires estimates of the branching ratios of the rare decay modes. For the $B^+ \rightarrow \mu^+ \mu^- K^+$ and $B^0 \rightarrow \mu^+ \mu^- K^{*0}$ decays we use the world average measured branching ratios [23], while for $B_s^0 \rightarrow \mu^+ \mu^- \phi$ we use the theoretical estimate [15]. The expected number of background events N_{bkg} is estimated by extrapolating the candidate yield with an invariant mass (180–300) MeV/c^2 higher than the B mass, to the signal region. Candidates with an invariant mass lower than the B mass are not suitable for background estimates, since they contain partially reconstructed B decays, not expected in the signal region. We find good discriminating power between signal and background from the following three quantities: t/σ_t ,

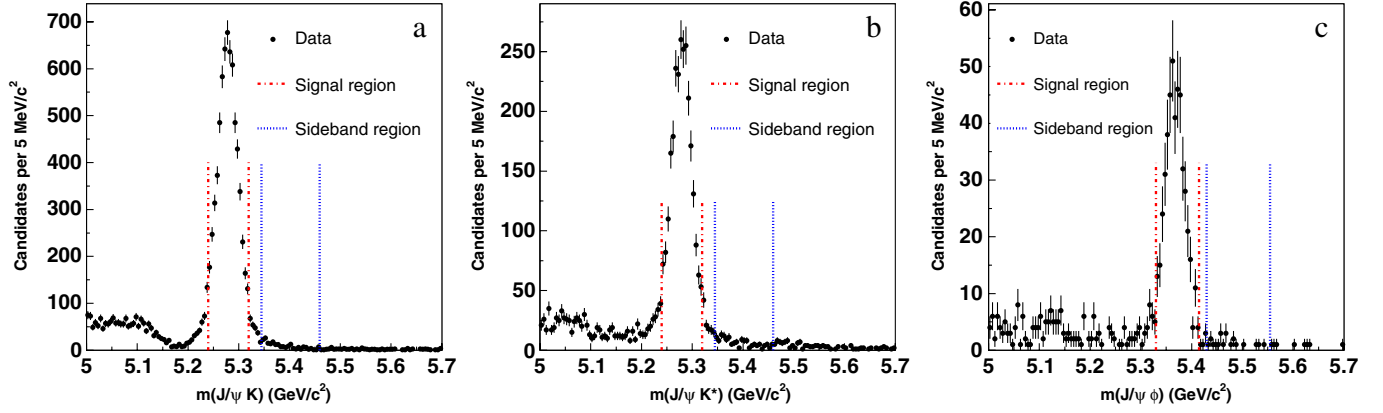


FIG. 1 (color online). Invariant mass spectra of (a) $J/\psi K^+$, (b) $J/\psi K^{*0}$, and (c) $J/\psi \phi$ candidates after applying optimized selection requirements.

α , and I . The significance of the proper decay time t/σ_t is defined as the proper decay time of the B candidate, divided by its uncertainty. The angle α is defined as the difference in angle between the B candidate's momentum vector and the vector from the primary vertex to the $\mu\mu h$ vertex. The isolation I is defined as the transverse momentum carried by the B meson candidate divided by the transverse momentum of all tracks in a cone of $\Delta R = \sqrt{\Delta\eta^2 + \Delta\phi^2} = 1.0$ around the direction of the B meson candidate, including those of the B candidate itself. Here $\Delta\eta$ is the difference in pseudorapidity of the B candidate and each track, and $\Delta\phi$ is the difference in their azimuthal angles. Scanning different combinations of selection thresholds, we find that the optimal values are very similar for the three rare decay modes: $t/\sigma_t \geq 14$, $\alpha \leq 60$ mrad, and $I \geq 0.6$. Applying the optimized selection requirements to the normalization channels yields the distributions shown in Fig. 1. The shape of the combinatoric background is estimated from a sample with poor vertex quality (χ^2 probability $< 10^{-3}$). The invariant mass distri-

bution of this poor vertex quality sample is fitted with a Gaussian distribution for the remaining signal contribution and an exponential plus a constant to model the background. We estimate the background in the signal region of the tight selection using this functional form, normalized to the number of candidates with invariant mass (60 – 180) MeV/c^2 higher than the B mass. Using this method, we find $6361 \pm 82 B^+ \rightarrow J/\psi K^+$, $2423 \pm 52 B^0 \rightarrow J/\psi K^{*0}$, and $431 \pm 22 B_s^0 \rightarrow J/\psi \phi$ decays. The invariant mass distributions for the rare decay modes are shown in Fig. 2. In the ± 40 MeV/c^2 window around the B mass we find $90 B^+ \rightarrow \mu^+ \mu^- K^+$, $35 B^0 \rightarrow \mu^+ \mu^- K^{*0}$, and $11 B_s^0 \rightarrow \mu^+ \mu^- \phi$ candidates. From simulation studies we verified that the present selection accepts decays for every kinematically possible dimuon invariant mass, with an efficiency difference not exceeding a factor two, except for the windows around the $J/\psi^{(\prime)}$ that have been explicitly excluded.

For the signal modes, we evaluate three sources of background: the combinatoric background, hadrons misidentified as muons, and hadrons with misassigned mass.

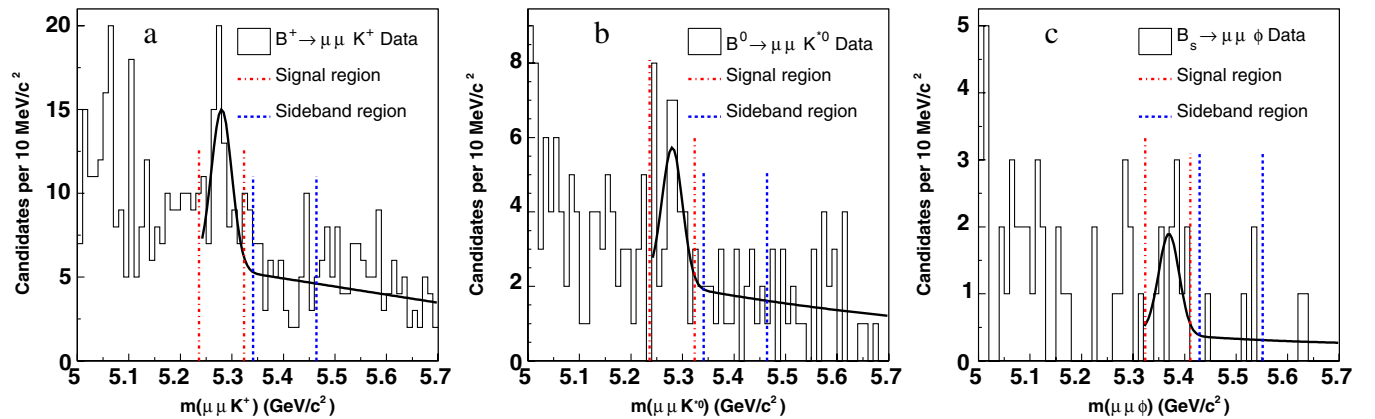


FIG. 2 (color online). Invariant mass spectra of (a) $\mu^+ \mu^- K^+$, (b) $\mu^+ \mu^- K^{*0}$, and (c) $\mu^+ \mu^- \phi$ candidates. The superimposed curves are not a fit, but a sum of a single Gaussian with a width of 20 MeV/c^2 representing the signal, and a curve representing the background as determined by the procedure described in the text. The curves are not drawn for masses below the signal window since they are not expected to predict the background level where partially reconstructed B decays contribute.

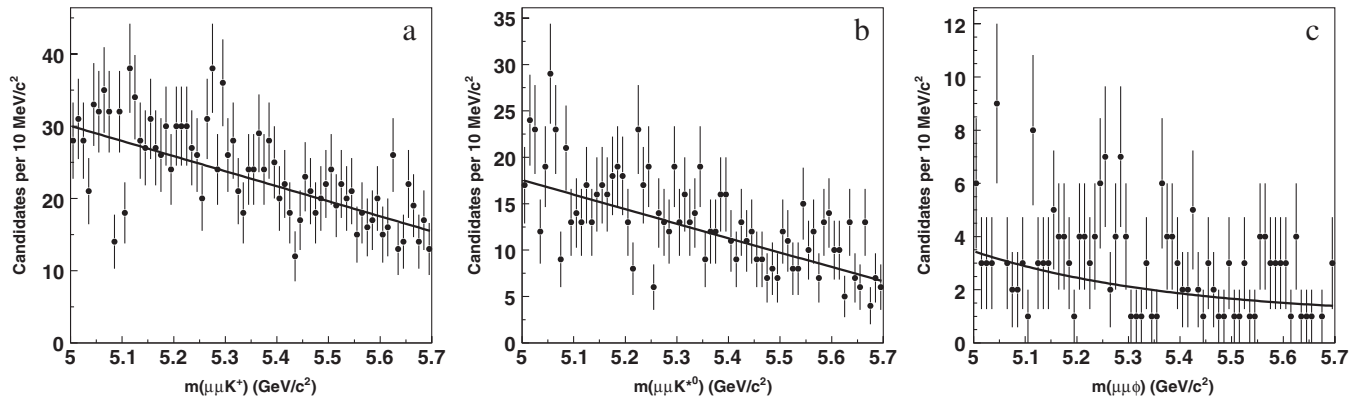


FIG. 3. Invariant mass spectra of samples used for determining the background shapes for (a) $\mu^+\mu^-K^+$, (b) $\mu^+\mu^-K^{*0}$, and (c) $\mu^+\mu^-\phi$ candidates. The selections differ from those used for Fig. 2, in that the selection on the vertex quality requirement has been inverted: χ^2 probability $<10^{-3}$. Superimposed is a curve that represents the fit to an exponential plus a constant.

As in the normalization mode, the shape of the combinatoric background is estimated from a sample with poor vertex quality (χ^2 probability $<10^{-3}$). The invariant mass distribution of these candidates is fitted to an exponential plus a constant, shown in Fig. 3. This functional form is used to extrapolate the number of candidates with invariant mass (60–180) MeV/c^2 higher than the B mass to the signal region. The resulting backgrounds, and their statistical uncertainties, consist of 44.3 ± 5.8 , 16.3 ± 3.6 , and 3.1 ± 1.5 candidates for the $B^+ \rightarrow \mu^+\mu^-K^+$, $B^0 \rightarrow \mu^+\mu^-K^{*0}$, and $B_s^0 \rightarrow \mu^+\mu^-\phi$ decay modes, respectively. The statistical error on the fitted parameters from the background sample is included in the quoted error. Backgrounds from hadrons misidentified as muons are estimated from simulation. Final state particles from simulated charmless B decays are weighted with the muon misidentification probabilities. The misidentification probabilities for charged kaons and pions are measured from a sample of $D^{*+} \rightarrow D^0\pi^+$ followed by $D^0 \rightarrow K^-\pi^+$ decays. We estimate a net background of 1.0 events for the $B^+ \rightarrow \mu^+\mu^-K^+$ channel, primarily coming from misidentified $B^+ \rightarrow K^+\pi^-\pi^+$ decays. For the B^0 and B_s^0 modes, this background is negligible. From simulation we determine the background contribution that arises from assigning the wrong masses to the hadrons. We estimate $0.4B^0 \rightarrow \mu^+\mu^-K^{*0}$ decays which are reconstructed as $B_s^0 \rightarrow \mu^+\mu^-\phi$ and $0.2B_s^0 \rightarrow \mu^+\mu^-\phi$ decays reconstructed as $B^0 \rightarrow \mu^+\mu^-K^{*0}$. Nonresonant contributions in the K^{*0} region have been measured in radiative decays to be $\approx 1\%$ [28], and we neglect them as a potential background.

We calculate the signal yield by subtracting the predicted background from the number of candidates in the signal window. We find an excess in the B signal region in all three channels, and determine the significance by calculating the Poisson probability for the background to fluctuate to the number of observed events or higher, taking into account the statistical and systematic uncertainty on

the background. We find an equivalent Gaussian significance of 4.5, 2.9, and 2.4 standard deviations, respectively, for the B^+ , B^0 , and B_s^0 modes.

Table I lists the systematic uncertainties associated with the relative selection efficiency, discussed in further detail below. To take into account the uncertainty on the relative efficiency due to uncertainties in the dynamics of the rare decays, we apply the weak form factors from Ref. [29,30] and evaluate the largest difference between the reconstruction efficiency and the central value. We find an uncertainty of 3.1% or less. The uncertainty related to the $p_T(B)$ spectrum is evaluated from the change in relative efficiency when the three parameters in the $p_T(B)$ weighting function are varied by 1 standard deviation of their values determined from fits to data, taking into account correlations. The difference reaches 1.4% in the B_s^0 mode. The muon trigger efficiency close to the 1.5 GeV/c p_T threshold is poorly known. We find a change in the relative efficiency reaching 1.3% if the minimum p_T is varied by ± 100 MeV/c , covering the range over which the trigger efficiency rises from zero to one. The final state particles of the rare decay modes have approximately 10% more low momentum tracks than those of the normalization chan-

TABLE I. Systematic uncertainties on the relative efficiency quoted in percent.

Channel	B^+	B^0	B_s
Theory model	1.5	3.1	1.6
$p_T(B)$ spectrum	0.6	1.3	1.4
Trigger turn-on	1.3	1.3	1.2
Low momentum hadrons	0.2	0.2	0.2
B_s^0 decay width difference	8.7
Polarization	...	0.6	0.1
Normalization channel statistics	1.3	2.1	5.1
$B^+ \rightarrow J/\psi\pi^+$ contribution	0.1
MC statistics	1.6	2.6	2.2
Total	2.9	5.0	10.6

TABLE II. Summary of systematic uncertainties quoted in percent.

Channel	B^+	B^0	B_s
Total relative efficiency uncertainty	2.9	5.0	10.6
$\mathcal{B}(J/\psi \rightarrow \mu^+ \mu^-)$	1.0	1.0	1.0
Background prediction	5.2	3.1	10.2
$\mathcal{B}(B \rightarrow J/\psi h)$	3.5	4.5	35.5

nels. The simulation models the track reconstruction efficiency to an accuracy of 2% in the p_T range of 0.4–1.5 GeV/ c . We therefore assign a systematic uncertainty on the relative efficiency of $2\% \times 10\% = 0.2\%$. We find an uncertainty of 8.3% on the relative efficiency of B_s^0 decays due to the unknown fraction of the short-lived CP -even state in the rare decay mode. We assume that the CP -even fraction is 0.5, and assess systematic uncertainties for the extremes of the fraction valued at 1.0 and 0.0. In addition, the uncertainty on $\Delta\Gamma/\Gamma$ contributes another 2.6%, resulting in a total uncertainty of 8.7% associated with the B_s^0 decay width difference. This is the largest systematic uncertainty on the relative efficiency of the B_s^0 mode. We evaluate the effect of the uncertainty on the fraction of J/ψ mesons produced with a longitudinal polarization by varying the fraction measured at CDF [26] by $\pm 1\sigma$. The effect is 0.6% for $B^0 \rightarrow J/\psi K^{*0}$ and 0.1% for $B_s^0 \rightarrow J/\psi \phi$.

The statistical uncertainties of yields in the normalization channels are included as systematic uncertainties, which range from 1.3% for the B^+ channel to 5.1% for the B_s^0 channel. Cabibbo-suppressed $B^+ \rightarrow J/\psi \pi^+$ decays contribute 0.1% to the yield of the normalization channel for the B^+ channel. We introduce the full effect into our estimate of the systematic uncertainty without correcting the result. The relative efficiencies between signal and normalization channels, of 0.71 ± 0.01 , 0.74 ± 0.02 , and 0.84 ± 0.02 for the B^+ , B^0 , and B_s^0 decays, respectively, have uncertainties reaching 2.6%, that arise from the finite size of the MC samples.

The predicted background values depend on the shape of the background function. We evaluate the change in the background yield calculation when using a sample that is similar to the one resulting from the optimal selection, but has less stringent requirements on the three optimization variables instead of the default sample with poor vertex quality. We compare two functional models for the background description, the default exponential plus a constant, and a simpler linear extrapolation function. We find a systematic uncertainty on the background prediction reaching 10% for the B_s^0 channel.

To calculate the systematic uncertainty on the relative branching fraction, the relative efficiency uncertainty is summed in quadrature with the uncertainty of the $J/\psi \rightarrow \mu^+ \mu^-$ branching ratio, and with the systematic uncertainty on the number of signal candidates.

To calculate the absolute branching fractions, we use the world average branching fractions of the normalization channels [23]. These branching fractions have uncertainties of 3.5%, 4.5%, and 35.5%, respectively, for B^+ , B^0 , and B_s^0 , which are added in quadrature to the systematic uncertainties on the relative branching ratios. A summary of the systematic uncertainties is given in Table II.

We calculate relative branching ratios using Eq. (1), and find $\mathcal{B}(B^+ \rightarrow \mu^+ \mu^- K^+)/\mathcal{B}(B^+ \rightarrow J/\psi K^+) = (0.59 \pm 0.15 \pm 0.03) \times 10^{-3}$, $\mathcal{B}(B^0 \rightarrow \mu^+ \mu^- K^{*0})/\mathcal{B}(B^0 \rightarrow J/\psi K^{*0}) = (0.61 \pm 0.23 \pm 0.07) \times 10^{-3}$, and $\mathcal{B}(B_s^0 \rightarrow \mu^+ \mu^- \phi)/\mathcal{B}(B_s^0 \rightarrow J/\psi \phi) = (1.23 \pm 0.60 \pm 0.14) \times 10^{-3}$, where the first uncertainty is statistical and the second is systematic. We use the world average branching ratios of the B^0 and B^+ normalization channels [23], resulting in the following absolute branching fractions: $\mathcal{B}(B^+ \rightarrow \mu^+ \mu^- K^+) = (0.59 \pm 0.15 \pm 0.04) \times 10^{-6}$ and $\mathcal{B}(B^0 \rightarrow \mu^+ \mu^- K^{*0}) = (0.81 \pm 0.30 \pm 0.10) \times 10^{-6}$. To obtain an absolute branching ratio for the $B_s^0 \rightarrow \mu^+ \mu^- \phi$ decay, we use $\mathcal{B}(B_s^0 \rightarrow J/\psi \phi) = (1.38 \pm 0.49) \times 10^{-3}$, obtained from correcting the CDF measurement [31] for the current value of f_s/f_d [23], the B_s^0 to B^0 production ratio, resulting in $\mathcal{B}(B_s^0 \rightarrow \mu^+ \mu^- \phi) = (1.70 \pm 0.82 \pm 0.64) \times 10^{-6}$. We find a significance of only 2.4 standard

TABLE III. Summary of the main ingredients and results of this analysis. Where one uncertainty is quoted, the uncertainty is of statistical nature. Where two uncertainties are quoted, the first is statistical and the second is systematic.

Decay mode	$B^+ \rightarrow \mu^+ \mu^- K^+$	$B^0 \rightarrow \mu^+ \mu^- K^{*0}$	$B_s^0 \rightarrow \mu^+ \mu^- \phi$
N_{obs}	90	35	11
N_{bkg}	45.3 ± 5.8	16.5 ± 3.6	3.5 ± 1.5
N_{sig}	44.7 ± 5.8	18.5 ± 3.6	7.5 ± 1.5
Gaussian significance	4.5σ	2.9σ	2.4σ
$N_{J/\psi h}$	6361 ± 82	2423 ± 52	431 ± 22
$\epsilon_{\mu^+ \mu^- h}/\epsilon_{J/\psi h}$	0.71 ± 0.01	0.74 ± 0.02	0.84 ± 0.02
Relative $\mathcal{B} \times 10^3$	$0.59 \pm 0.15 \pm 0.03$	$0.61 \pm 0.23 \pm 0.07$	$1.23 \pm 0.60 \pm 0.14$
Absolute $\mathcal{B} \times 10^6$	$0.59 \pm 0.15 \pm 0.04$	$0.81 \pm 0.30 \pm 0.10$	$1.70 \pm 0.82 \pm 0.64$
Relative \mathcal{B} 95(90)% CL limit $\times 10^3$	2.6(2.3)
Absolute \mathcal{B} 95(90)% CL limit $\times 10^6$	6.0(5.0)

deviations for the $B_s^0 \rightarrow \mu^+ \mu^- \phi$ decay mode. Therefore, we choose to set a limit on this decay. We use a Bayesian integration assuming a flat prior [32], and find $\mathcal{B}(B_s^0 \rightarrow \mu^+ \mu^- \phi) / \mathcal{B}(B_s^0 \rightarrow J/\psi \phi) < 2.6(2.3) \times 10^{-3}$ at the 95 (90)% confidence level (CL). We also set an upper limit on the absolute branching ratio, taking into account the uncertainty of the branching ratio of the normalization channel [33]. We assume that the prior probability density function representing the uncertainty in the normalization channel is a log normal distribution with a mean equal to the central value, and a width parameter equal to the quoted uncertainty of 35.5%. We obtain $\mathcal{B}(B_s^0 \rightarrow \mu^+ \mu^- \phi) < 6.0(5.0) \times 10^{-6}$ at 95(90)% CL. The main ingredients and the results are summarized in Table III.

In conclusion, our measurements of the B^+ and B^0 rare decay modes are consistent with the SM predictions, and with previous measurements [5,6]. The relative limit on $B_s^0 \rightarrow \mu^+ \mu^- \phi$ is consistent with the SM predictions, and is the most stringent to date.

We thank the Fermilab staff and the technical staffs of the participating institutions for their vital contributions. This work was supported by the U.S. Department of Energy and National Science Foundation; the Italian Istituto Nazionale di Fisica Nucleare; the Ministry of Education, Culture, Sports, Science and Technology of Japan; the Natural Sciences and Engineering Research Council of Canada; the National Science Council of the Republic of China; the Swiss National Science Foundation; the A.P. Sloan Foundation; the Bundesministerium für Bildung und Forschung, Germany; the Korean Science and Engineering Foundation and the Korean Research Foundation; the Science and Technology Facilities Council and the Royal Society, UK; the Institut National de Physique Nucleaire et Physique des Particules/CNRS; the Russian Foundation for Basic Research; the Comisión Interministerial de Ciencia y Tecnología, Spain; the European Community's Human Potential Programme; the Slovak R&D Agency; and the Academy of Finland.

-
- [1] P. Colangelo, F. De Fazio, R. Ferrandes, and T.N. Pham, Phys. Rev. D **73**, 115006 (2006).
- [2] F. Kruger and J. Matias, Phys. Rev. D **71**, 094009 (2005).
- [3] T.M. Aliev, A. Ozpineci, and M. Savci, Eur. Phys. J. C **29**, 265 (2003).
- [4] D. A. Demir, K. A. Olive, and M. B. Voloshin, Phys. Rev. D **66**, 034015 (2002).
- [5] B. Aubert *et al.* (BABAR Collaboration), Phys. Rev. D **73**, 092001 (2006).
- [6] A. Ishikawa *et al.* (Belle Collaboration), Phys. Rev. Lett. **91**, 261601 (2003).
- [7] G. Burdman, Phys. Rev. D **52**, 6400 (1995).
- [8] P. Colangelo, F. De Fazio, P. Santorelli, and E. Scrimieri, Phys. Rev. D **53**, 3672 (1996); **57**, 3186(E) (1998).
- [9] T.M. Aliev, A. Ozpineci, and M. Savci, Phys. Rev. D **56**, 4260 (1997).
- [10] D. Melikhov, N. Nikitin, and S. Simula, Phys. Rev. D **57**, 6814 (1998).
- [11] A. Ali, P. Ball, L. T. Handoko, and G. Hiller, Phys. Rev. D **61**, 074024 (2000).
- [12] H.M. Choi, C.R. Ji, and L.S. Kisslinger, Phys. Rev. D **65**, 074032 (2002).
- [13] A. Ali, E. Lunghi, C. Greub, and G. Hiller, Phys. Rev. D **66**, 034002 (2002).
- [14] C.H. Chen and C.Q. Geng, Phys. Rev. D **66**, 094018 (2002).
- [15] C.Q. Geng and C.C. Liu, J. Phys. G **29**, 1103 (2003).
- [16] V.M. Abazov *et al.* (D0 Collaboration), Phys. Rev. D **74**, 031107 (2006).
- [17] D. Acosta *et al.* (CDF Collaboration), Phys. Rev. D **65**, 111101 (2002).
- [18] D. Acosta *et al.* (CDF Collaboration), Phys. Rev. D **71**, 032001 (2005).
- [19] A. Sill *et al.*, Nucl. Instrum. Methods Phys. Res., Sect. A **447**, 1 (2000).
- [20] A.A. Affolder *et al.*, Nucl. Instrum. Methods Phys. Res., Sect. A **526**, 249 (2004).
- [21] G. Ascoli *et al.*, Nucl. Instrum. Methods Phys. Res., Sect. A **268**, 33 (1988).
- [22] The CDF reference frame uses cylindrical coordinates, where θ and ϕ are the polar and azimuthal angles with respect to the proton beam. Pseudorapidity η is defined as $-\ln(\tan(\theta/2))$.
- [23] W.-M. Yao *et al.*, J. Phys. G **33**, 1 (2006).
- [24] D.J. Lange, Nucl. Instrum. Methods Phys. Res., Sect. A **462**, 152 (2001).
- [25] I. Dunietz, R. Fleischer, and U. Nierste, Phys. Rev. D **63**, 114015 (2001).
- [26] D. Acosta *et al.* (CDF Collaboration), Phys. Rev. Lett. **94**, 101803 (2005).
- [27] R. Brun *et al.*, CERN Program Library Long Writup W5013, 1994.
- [28] M. Nakao *et al.* (Belle Collaboration), Phys. Rev. D **69**, 112001 (2004).
- [29] D. Melikhov and B. Stech, Phys. Rev. D **62**, 014006 (2000).
- [30] P. Colangelo, F. De Fazio, and P. Santorelli, Phys. Rev. D **51**, 2237 (1995).
- [31] F. Abe *et al.* (CDF Collaboration), Phys. Rev. D **54**, 6596 (1996).
- [32] J. Heinrich, C. Blocker, J. Conway, L. Demortier, L. Lyons, G. Punzi, and P.K. Sinervo, arXiv:physics/0409129.
- [33] Note that the uncertainty in the normalization mode's branching ratio was not taken into account in [16].